Environmental Pollution 251 (2019) 238–245

Contents lists available at ScienceDirect

Environmental Pollution

journal homepage: www.elsevier.com/locate/envpol

Nanobody-based fluorescence resonance energy transfer immunoassay for noncompetitive and simultaneous detection of ochratoxin a and ochratoxin B★

Zongwen Tang [a, 1], Xing Liu [a, *, 1], Yuanyuan Wang [a], Qi Chen [a], Bruce D. Hammock [b], Yang Xu [c]

[a] College of Food Science and Engineering, Hainan University, 58 Renmin Avenue, Haikou, 570228, PR China
[b] Department of Entomology and Nematology and UCD Comprehensive Cancer Center, University of California, Davis, CA, 95616, United States
[c] State Key Laboratory of Food Science and Technology, Nanchang University, 235 Nanjing East Road, Nanchang, 330047, PR China

ARTICLE INFO

Article history:
Received 27 February 2019
Received in revised form
26 April 2019
Accepted 29 April 2019
Available online 2 May 2019

Keywords:
Nanobody
Mycotoxin
Fluorescence resonance energy transfer
Immunoassay

ABSTRACT

A noncompetitive and homogeneous fluorescence resonance energy transfer (FRET) immunoassay was developed using a nanobody (Nb) for highly sensitive and simultaneous detection of ochratoxin A (OTA) and ochratoxin B (OTB). The promoted intrinsic fluorescence (λ_{ex}: 280 nm) of tryptophan residues (donor) in Nb can excite the fluorescence of OTA and OTB (acceptor) for detection (λ_{em}: 430 nm). Using optimal conditions, the limits of detection of the Nb-based FRET immunoassay were 0.06 and 0.12 ng/mL for OTA and OTB, respectively. Minimal cross reactivity was detected for several analogues of OTA and OTB as well as nonspecific proteins and antibodies. Acceptable accuracy and precision were obtained in the spike and recovery study, and the results correlated well with those by HPLC. These results demonstrated that the developed method could be a useful tool for noncompetitive, homogeneous, and simultaneous detection of OTA and OTB as well as other environmental analytes with similar fluorescence properties.

1. Introduction

Mycotoxins are the secondary metabolites of various fungi, and have become a major threat to food safety because of their toxic effects and wide distribution in the world. Ochratoxins (OTs) are a group of mycotoxins produced by several species of *Aspergillus* and *Penicillium* (Gareis and Gareis, 2007). OTs mainly contain three analogues, ochratoxin A (OTA), ochratoxin B (OTB), and ochratoxin C (OTC), of which OTB and OTC are the non-chlorinated and ethyl ester of OTA, respectively. OTs have effects of nephrotoxicity, hepatotoxicity, immunotoxicity, teratogenicity, cytotoxicity, and genotoxicity on humans and animals (Gan et al., 2018; Lee et al., 2019; Tao et al., 2018). The toxicities of these molecules are attributed to the isocoumarin moiety and the lactone carbonyl group in their structures (Xiao et al., 1996). Currently many countries and organizations have set up the maximum limit of OTA in food because of its high portion in total OTs contamination, and various methods have been developed for OTA detection. Due to the toxicities of natural analogues of OTA, it is necessary to attach importance to their detection although no maximum limits have been established for them.

Various chromatography detection methods have been established for OTs, such as high performance liquid chromatography and liquid chromatography tandem mass spectrometry (Al-Taher et al., 2017; Campone et al., 2018; Di Stefano et al., 2015). The chromatography methods exhibit high sensitivity and good reliability. However, they are limited for the expensive instruments, time-consuming pretreatment of sample, and laborious operation. Immunoassays are selected as an alternative to chromatography methods because of the advantages of low cost, ease operation, and high sensitivity. The reported immunoassays for OTs are mainly performed in the competitive and heterogeneous format (Liang et al., 2016; Liu et al., 2017; Liu et al., 2015; Liu et al., 2014; Qileng et al., 2018; Sun et al., 2017; Sun et al., 2018; Sun et al., 2019; Tang et al., 2018). Moreover, various protocols were used to

★ This paper has been recommended for acceptance by Charles Wong.
* Corresponding author.
E-mail address: xliu@hainanu.edu.cn (X. Liu).
[1] These authors contributed equally to this work.

https://doi.org/10.1016/j.envpol.2019.04.135
0269-7491/

improve the detection limit of immunoassays for low molecular weight compounds in the noncompetitive and heterogeneous format, such as PHAIA-based immunoassay and open sandwich immunoassay (Kim et al., 2011; Lim et al., 2007). Nevertheless, the improvement of detection sensitivity of these methods are still restricted due to the heterogeneous assay format that involves repetitive steps of incubation and washing.

Fluorescence resonance energy transfer (FRET) is a process in which the electronic excited state energy transfer occurs between two chromophores, namely the donor and the acceptor, respectively (Masters, 2014). The FRET results in light emission from the acceptor when the distance between the excited donor and acceptor ranges from 1 to 10 nm (Tyagi et al., 2000). FRET is a homogeneous reaction system and thus the combination of FRET and immunoassay can efficiently improve the detection limit of immunoassay and shorten the assay time by eliminating repetitive steps of incubation and washing. Most current FRET-based immunoassay systems require fluorescent dyes or fluorophore-tagged antibodies and antigens to act as donors and acceptors. Since the antibody has intrinsic fluorescence resulting from the indigenous tryptophan (Trp) residues (λ_{ex}: 280 nm and λ_{em}: 350 nm), the antibody can serve as a donor in FRET interactions with bound ligands or antigens participating as acceptors (Borkman and Lerman, 1978; Li et al., 2013). Consequently, the specific binding of an antibody to an antigen can lead to fluorescence quenching of Trp residues in the antibody and fluorescence enhancement of the antigen which involves the energy transfer efficiency. According to Förster's theory, the energy transfer efficiency can be increased by shortening the distance between the donor and acceptor (effective FRET distance, *R*) (Lakowicz, 1999). Compared to the intact antibody, an antigen-binding fragment (Fab) contains a higher proportion of Trp residues that are close to the bound target antigen. Since the fluorescence efficiency mainly depends on Trp residues in the variable domains of an antibody, the FRET immunoassay using an Fab shows more intense fluorescence quenching by the bound target antigen (Schreiber et al., 1978). This phenomenon was validated by the theoretically calculated values of *R* for intact antibody-antigen and Fab-antigen (Li et al., 2013). Thus, the utilization of a miniaturized antibody to replace the intact antibody in FRET immunoassay is an effective approach to shorten the effective FRET distance by decreasing the mean distance between Trp residues and antigen binding site, and improve the energy transfer efficiency for a lower detection limit.

With the rapid development of antibody engineering and molecular cloning techniques, numerous genetically engineered antibodies have been explored, such as single chain variable fragments and nanobodies (Nbs). The Nbs have a molecular weight of approximately 12–15 kDa and are reported to be the smallest intact antigen-binding single polypeptide chains in natural antibodies (Muyldermans, 2013). Nbs are derived from heavy-chain antibodies (HCAbs) and new antigen acceptors (NARs), which are naturally devoid of light chains and present in camelids and sharks (Greenberg et al., 1995; Hamers-Casterman et al., 1993). Both the HCAbs and NARs have an antigen recognition part composed of single variable domains, considered as the variable domain of the heavy chain of HCAb (VHH) and of the NAR (V-NAR) (Harmsen and De Haard, 2007; Muyldermans, 2013). Owing to the cylindrical shape of 2.5 nm diameter and 4 nm height, these single variable domains are accordingly named as Nbs by its original developer Ablynx and sometimes more generally referred to as VHH. Due to the advantages of ease expression, high solubility, and high tolerance to harsh environment, various Nbs have been developed to replace intact antibodies for competitive and heterogeneous detection of compounds with low molecular weight, including mycotoxins, pesticides, and other contaminants in food and environment (Bever et al., 2014; He et al., 2014; Huo et al., 2018; Sun et al., 2018; Wang et al., 2014). Nevertheless, there are few reports on the development of noncompetitive and homogeneous immunoassays for low molecular weight compounds using Nbs.

In previous work, we reported the development of alpaca anti-OTA Nbs and a sensitive indirect competitive Nb-based ELISA for OTA with an LOD of 0.16 ng/mL (Liu et al., 2017; Liu et al., 2014). To evaluate the potential of Nbs for improving assay sensitivity, the anti-OTA Nb (Nb28) was selected for establishing a FRET-based immunoassay system for noncompetitive and homogeneous detection of OTs in this study. The experimental parameters related to method optimization and evaluation are detailed. To our knowledge, a FRET-based immunoassay system using an Nb for noncompetitive, homogeneous, and simultaneous detection of OTs (OTA and OTB) and other analogues with low molecular weight has not yet been reported.

2. Materials and methods

2.1. Materials and instruments

Nickel-nitrilotriacetic acid (Ni-NTA) Sepharose was procured from Solarbio (Beijing, China). OTA, OTC, and fumonisin B_1 (FB_1) were obtained from Pribolab (Singapore). Aflatoxin B_1 (AFB_1) and zearalenone (ZEN) were purchased from Fermentek (Jerusalem, Israel). OTB was from Bioaustralis (Smithfield, NSW, Australia). Deoxynivalenol (DON) was from Sigma-Aldrich (CA, USA). Bovine serum albumin (BSA) and ovalbumin (OVA) were obtained from Sangon Biotech Inc. (Shanghai, China). The black microtiter plates were from Corning Inc. (NY, USA). The mouse anti-OTA monoclonal antibody mAb YK232 was obtained from Yikang Biotech Inc. (Haikou, China). The anti-alpha fetoprotein (AFP) Nb was prepared in our lab. The engineered BL21(DE3) strain of *E. coli* containing the vector Nb28-pET25b for Nb28 expression was prepared previously. All other chemicals and organic solvents were of reagent grade or better.

Fluorescence spectra and UV–vis spectra were obtained using a spectral scanning multimode reader SP-Max 3500FL (Flash Spectrum Inc., Shanghai, China). The HPLC system consisted of a Model E2695 pump, a Model 2475 fluorescence detector, and a SunFire C18 5 μm column (Waters, MA, USA).

2.2. Preparation of nanobody Nb28

The *E. coli* BL21(DE3) strain containing the vector Nb28-pET25b was used for auto-induction expression of the anti-OTA nanobody Nb28 according to previous work with some modifications (Liu et al., 2017). For pre-culture, 5 mL of LB medium containing ampicillin (100 μg/mL) was inoculated with a single colony and cultured overnight at 37 °C by shaking at 220 rpm. For the soluble expression of Nb28, 300 mL of auto-induction medium containing ampicillin (100 μg/mL) was inoculated with 3 mL of overnight culture, followed by 3 h of shaking culture at 37 °C. The expression of Nb28 was performed by vigorously shaking at 30 °C overnight. After centrifugation (10,000 g, 4 °C) for 30 min, the bacterial cells were collected from the culture and resuspended in 1 mL of lysis buffer (pH 8.0, 50 mM NaH_2PO_4, 300 mM NaCl, 10 mM imidazole) containing 1 mM PMSF and 1 mg/mL lysozyme per gram of wet weight. The cells were then subjected to ultrasonication, followed by centrifugation (10,000 g, 4 °C) for 15 min. The filtered supernatant flew through the protein purification column packed with Ni-NTA Sepharose by gravity. The column was washed with five column volumes of wash buffer (pH 8.0, 50 mM NaH_2PO_4, 300 mM NaCl, 20 mM imidazole) to remove nonspecifically bound proteins. Then 5 mL of elution buffer (pH 8.0, 50 mM NaH_2PO_4, 300 mM NaCl,

250 mM imidazole) was used for the competitive elution of bound Nb28. After protein dialysis against PBS (4 °C, 72 h), purity identification and quantification of the purified Nb28 were performed using the SDS-PAGE and the Bradford method, respectively. The purified Nb28 solution was frozen at −20 °C and used later.

2.3. Nb-based FRET immunoassay for OTA and OTB

The FRET immunoassay using Nb28 for simultaneous detection of OTA and OTB was performed as follows. Briefly, 180 μL of Nb28 solution (5 μg/mL in 0.01 M MES, pH 6.2) was mixed with 20 μL of OTA or OTB standard solution with various concentrations (0, 0.25, 0.5, 1.0, 2.0, 5.0, 10, 20, 50, and 100 ng/mL in 0.01 M MES containing 50% methanol) and added into the wells of black microtiter plate. After incubation at room temperature for 10 min, the fluorescence intensity (FI) at 430 nm of the mixture caused by FRET between Nb28 and analytes was recorded with the excitation wavelength at 280 nm. The quantitative analysis of OTA and OTB was performed according to the calibration curve for OTA, which was constructed by plotting the fluorescence enhancing rate (FE) against the logarithm of OTA concentrations. The FE was calculated with the following equation: $FE = (FI\text{-}FI_0)/FI_0$, where FI_0 and FI are the fluorescence intensity at 430 nm without and with the presence of analytes.

2.4. Selectivity of the Nb-based FRET immunoassay

In order to determine the selectivity of the Nb-based FRET immunoassay, the reactivity of the standard solutions of compounds (OTA, OTB, OTC, AB_1, ZEN, FB_1, and DON) with two concentrations (10 and 50 ng/mL) were tested with Nb28. Meanwhile, various proteins including 50 μg/mL BSA, 50 μg/mL OVA, 50 μg/mL mouse anti-OTA monoclonal antibody mAb YK232, and 5 μg/mL anti-AFP Nb were used to replace Nb28 for fluorescence detection.

2.5. Sample preparation and analysis

Rice samples for the Nb-based FRET immunoassay were prepared as shown below. Briefly, 0.2 g of ground sample was transferred to a 50 mL centrifuge tube containing 15 mL of 50% methanol-MES buffer. After 15 min of ultrasonic extraction, the sample mixture was centrifuged (8000 g, 4 °C) for 15 min. The supernatant was filtered through a 0.45 μm syringe filter before the Nb-based FRET immunoassay analysis. The filtrate was concentrated to dry under nitrogen and dissolved in methanol for analysis by HPLC with fluorescence detection (HPLC-FLD). Sample analysis by HPLC-FLD was performed as described by Remiro and coworkers with some modifications (Remiro et al., 2010). The mobile phase of HPLC-FLD contained acetonitrile and 0.4% formic acid solution. The proportions of acetonitrile:0.4% formic acid were 45:55 and 40:60 *(v/v)* for OTA and OTB at a flow rate of 1 mL/min, respectively. The injection volume was 20 μL, and the column temperature was maintained at 40 °C. The excitation and emission wavelengths of fluorescence detector were set at 333 and 460 nm for OTA and 318 and 460 nm for OTB, respectively.

2.6. Statistics analysis

Student's t-test was performed to assess the differences between the standard Nb-based FRET immunoassay calibration curves for OTA and OTB, between the standard Nb-based FRET immunoassay calibration curve for OTA in the optimal MES-MeOH buffer and those in rice sample matrix extracts with different dilution folds, and between the recovered OTs concentrations detected by the Nb-based FRET immunoassay and HPLC for each spiked level. The p-value was used to determine the significant differences.

3. Results and discussion

3.1. Expression, purification, and identification of the nanobody Nb28

The expression of nanobody Nb28 was assessed by SDS-PAGE (Figure S-1). Compared to the protein bands of the whole cells before auto-induction, a new band of 17 kDa for target protein Nb28 appeared in the whole cell protein of bacteria after auto-induction (Lanes 1 and 2). Moreover, the main form of the expressed Nb28 by auto-induction was soluble protein, since most of the target protein was found in the cell supernatant after ultrasonication (Lane 4). The Nb28 was separated from the supernatant of the broken cells by the Ni-NTA Sepharose affinity chromatography, and the purity identification of Nb28 was conducted by SDS-PAGE. A single clear band of 17 kDa was observed (Lane 5), which indicated that the Nb28 was well prepared with high purity. The yield of Nb28 was calculated to be 100 mg/L after quantification.

3.2. Construction of the Nb-based FRET immunoassay

As shown in Fig. 1, the Förster distance (R_0) and effective FRET distance (R) for intact antibody mAb YK232-OTA group (R_0: 23.24 Å, R: 27.2 Å) and Nb28-OTA group (R_0: 22.69 Å, R: 21.5 Å) were calculated according to the equations in the supporting material. Since the mean distance between Fc region of mAb YK232 and OTA is obviously longer than R_0 (23.24 Å), OTA-induced fluorescence quenching on Fc region Trp residues in mAb YK232 has an extremely low efficiency. Thus, the mAb YK232-OTA group has a bigger value of R than that of R_0. The Nb28-OTA group has a shorter effective FRET distance than that of the mAb YK232-OTA group, thus we hypothesized that the FRET immunoassay using Nb28 could show a higher energy transfer efficiency. To construct an Nb-based FRET immunoassay for noncompetitive and simultaneous detection of OTs, the fluorescence properties of Nb28 and OTs were

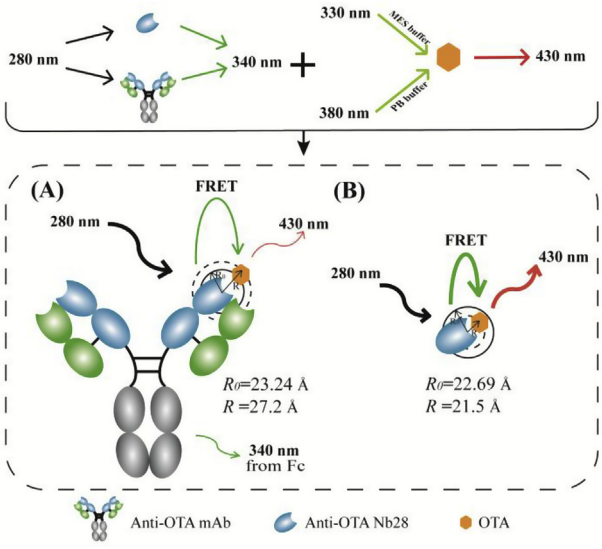

Fig. 1. Schematic illustration of the noncompetitive and homogeneous FRET immunoassay using intact antibody anti-OTA mAb YK232(A) and anti-OTA nanobody Nb28 (B), respectively. (R0: Förster distance; R: effective FRET distance).

investigated. The Nb28 contained two Trp residues in the previously reported amino sequence (Liu et al., 2014). Fluorescence spectrum scanning validation was performed by excitation at 280 nm to identify the fluorescence property of Nb28, and a significant fluorescence emission peak was observed at 325 nm (Fig. 2). There are three different prototropic forms (neutral, monoanion, and dianion) reported for OTA in solution, among which the monoanionic form and dianionic form dominate in acidic media and alkaline media, respectively (Il'ichev et al., 2001). It had been reported that the fluorescence emission peak at 450 nm for OTA was produced by excitation at ca. 330 nm in acidic media and ca. 380 nm in alkaline media, respectively (Hashemi and Alizadeh, 2009). Thus the fluorescence properties of OTA in solution varied significantly depending on its protonation state. The fluorescence spectra for OTs (OTA, OTB, and OTC) in MES buffer (0.01 M, pH 6.2) and PB buffer (0.01 M, pH 8.6) were scanned by excitation at 280 nm. The relative fluorescence intensity of emission at 430 nm in MES buffer was much lower than that in PB buffer (Fig. 2A and B), and thus MES buffer reduced the background signal. Moreover, the excitation spectra of OTA and OTB in MES buffer overlapped more with the emission spectrum of Nb28 than those in PB buffer did, which could enhance the detection signal (Fig. 2C and D). The MES buffer was selected because of the higher signal to noise ratio for improving the assay sensitivity. This was attributed to the high binding affinity between the dianions of OTA and OTB and Trp caused by electrostatic interaction (Il'ichev et al., 2002). Since no OTC dianion existed in acidic media, a low level of fluorescence intensity of OTC in MES buffer was observed by excitation at 280 nm (Fig. 2C). Thus the Nb-based FRET immunoassay was preliminarily constructed for simultaneous detection of OTA and OTB in MES buffer.

3.3. Optimization of the Nb-based FRET immunoassay

Effects of various conditions on the performance of the Nb-based FRET immunoassay was assessed, including immunoreaction time, pH, methanol, ionic strength, and surfactant (Figure S-2). The fluorescence enhancing rate of OTs (FE_{OTs}) caused by FRET from Nb28 (5 μg/mL) to OTs (100 ng/mL) was used for assessment criterion. The FE_{OTs} was calculated with the following equation: $FE_{OTs} = (FI_{Nb@OTs}\text{-}FI_{OTs})/FI_{OTA}$, where $FI_{Nb@OTs}$ and FI_{OTs} are the fluorescence intensity of OTA and OTB at 430 nm with and without the presence of Nb28 ($\lambda_{ex} = 280$ nm). The FE_{OTs} increased as the immunoreaction time increased, and there was no significant change when the time exceeded 10 min. Thus 10 min of immunoreaction time was selected for further research (Figure S–2A). Since the dianionic OTs exist in acidic media, the assay buffers with various pH (5.0–6.6) were tested. The FE_{OTs} increased from 2.16 to 2.69 when the pH ranged from 5.0 to 6.2. However, the FE_{OTA} significantly declined to 2.23 when the pH reached up to 6.6. Therefore, the pH of 6.2 was selected as the optimal one (Figure S–2B). Due to the hydrophobicity of OTA and OTB, it is necessary to use an organic reagent for the preparation of standard solutions and sample pretreatment. Methanol was commonly selected as the solvent of OTA and OTB, and the effect of methanol with various concentrations on assay performance was investigated (Figure S–2C). When the final concentration of methanol was no more than 5%, the FE_{OTs} gradually rose from 2.13 to 2.43. While a gradual decrease of the FE_{OTs} was observed when the methanol concentration increased from 5% to 20%. Hence, the recommended final concentration of methanol in assay buffer is 5%. To evaluate the effect of ionic strength on the Nb-based FRET immunoassay, the MES buffers (pH 6.2, 0.01 M) containing serial concentrations of

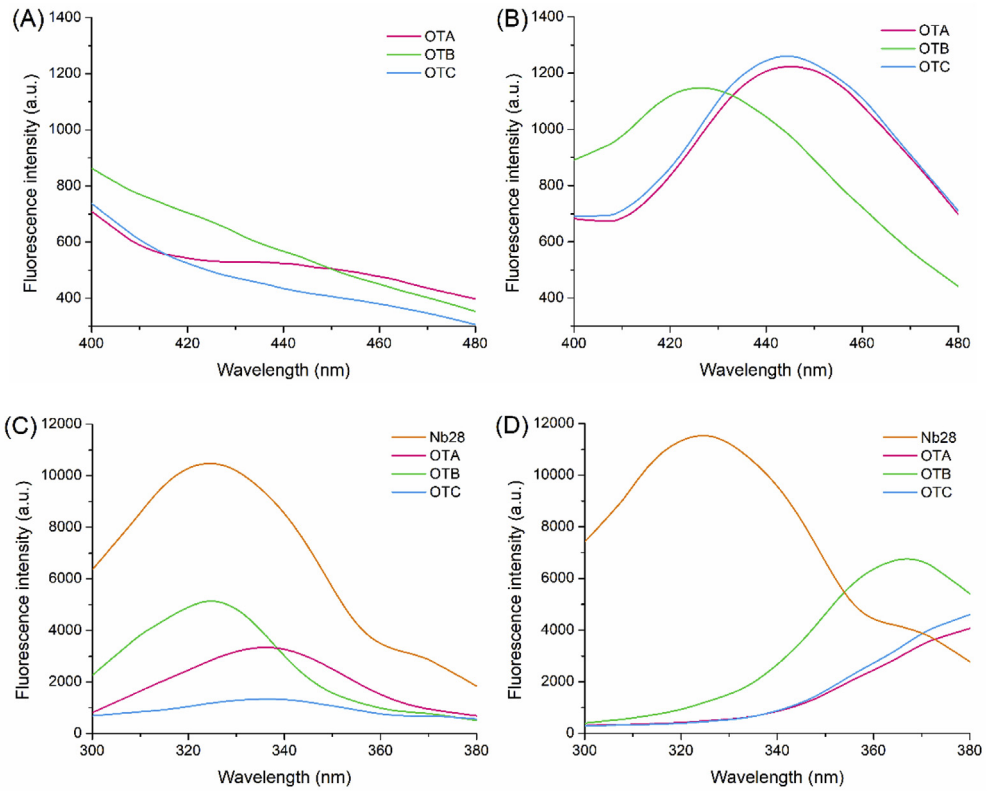

Fig. 2. Fluorescence emission spectra (λ_{ex}: 280 nm) of 100 ng/mL OTA, OTB and OTC in MES buffer (pH 6.2, 10 mM) (A) and PB buffer (pH 8.6, 10 mM) (B). Fluorescence emission spectra (λ_{ex}: 280 nm) of 5 μg/mL Nb28 and fluorescence excitation spectra (λ_{em}: 430 nm) of 100 ng/mL OTA, OTB, and OTC in MES buffer (C) and PB buffer (D). Both the MES buffer and PB buffer contain 0.5% Tween 20 and 5% methanol.

sodium chloride (0, 10, 25, 50, and 100 mM NaCl) were tested (Figure S–2D). Compared to the assay buffer with 0 mM NaCl, a significant decrease of FE_{OTs} was measured in assay buffers with higher content of NaCl. Thus the ionic strength of 0 mM was selected. Moreover, the assay buffers with various contents of nonionic surfactant Tween 20 were tested to reduce the nonspecific adsorption of Nb28-OTA immunocomplex by the microplate (Figure S–2E). The result showed that the addition of Tween 20 in assay buffer can effectively improve the relative fluorescence intensity compared to the MES buffer, and 0.05% of Tween 20 was selected for the highest FE_{OTs}. Under the optimal experimental conditions, the fluorescence emission spectra of Nb28 (5 μg/mL, $\lambda_{em} = 324$ nm) and the UV absorption spectra of OTA (100 μg/mL, $\lambda_{ab} = 333$ nm) and OTB (100 μg/mL, $\lambda_{ab} = 320$ nm) were measured (Figure S–2F). The UV absorption spectra of both analytes overlapped well with the normalized fluorescence emission spectra of Nb28, which ascertained the FRET from Nb28 to OTA and OTB.

Furthermore, fluorescence spectra of the mixture of Nb28 (5 μg/mL) and serial concentrations (0, 0.25, 0.5, 1, 2, 5, 10, 20, 50, and 100 ng/mL) of the analytes (OTA and OTB) were scanned (Fig. 3A and B). As the concentration of OTA and OTB increased, significant and similar fluorescence intensity decrease (wavelength = 330 nm) and increase (wavelength = 430 nm) was observed for both analytes. This phenomenon was attributed to energy transferring of the intrinsic fluorescence quenching of Nb28 caused by the FRET between Nb28 and analytes. Moreover, the fluorescence enhancing efficiency correlated well with the concentration of OTA and OTB ranging from 0.25 ng/mL to 20 ng/mL (Insets in Fig. 3C and D). At 95% confidence level, no significant difference was observed between the standard calibration curves of Nb-based FRET immunoassay for OTA and OTB using the Student's t-test analysis ($p > 0.05$). Thus, the calibration curve for OTA was applicable to OTB. The limit of detection (LOD) of the Nb-based FRET immunoassay was calculated to be 0.06 ng/mL for OTA and 0.12 ng/mL for OTB, and the LOD equals to the average response of 20 blank samples minus 3-fold standard deviations (Xu et al., 2014). The LOD of OTA by the Nb-based noncompetitive homogeneous FRET immunoassay was improved 2.7 folds compared to that (0.16 ng/mL) by the Nb-based indirect competitive heterogeneous ELISA (Liu et al., 2017). Besides, the assay time (10 min) of the developed FRET immunoassay was 7 folds shorter than that (70 min) of the Nb-based indirect competitive heterogeneous ELISA (Liu et al., 2017). Moreover, the analytical performance of the Nb-based FRET immunoassay was compared with other nanotechnology- and mass spectrometry-based assays for OTs (Campone et al., 2018; He et al., 2019; Meerpoel et al., 2018; Qileng et al., 2018; Rodríguez-Cabo et al., 2016). The detection limits for those nanotechnology- and mass spectrometry-based assays are often lower, but they are limited by the time-consuming operation and expensive equipments (Table 1). In contrast, the mouse anti-OTA monoclonal antibody (mAb YK232, 50 μg/mL) was used to replace Nb28 for FRET immunoassay (Fig. 4A). The mAb YK232 showed a higher fluorescence intensity at the wavelength of 330 nm than Nb28 because of more Trp residues in mAb YK232 (Inset in Fig. 4A). However, the stronger fluorescence intensity at the wavelength of 430 nm was tested in the Nb28@OTA (100 ng/mL) FRET immunoassay system than in the mAb@OTA (100 ng/mL) group (Inset in Fig. 4A). This can be ascribed to the fact that the former has a higher energy transfer efficiency (45%) than the latter (15%). Thus, the higher fluorescence enhancing efficiency was obtained in both Nb28@OTA and Nb28@OTB groups than in mAb YK232@OTA group (Fig. 4A). Moreover, the LOD of mAb YK232-based FRET immunoassay for OTA was calculated to be

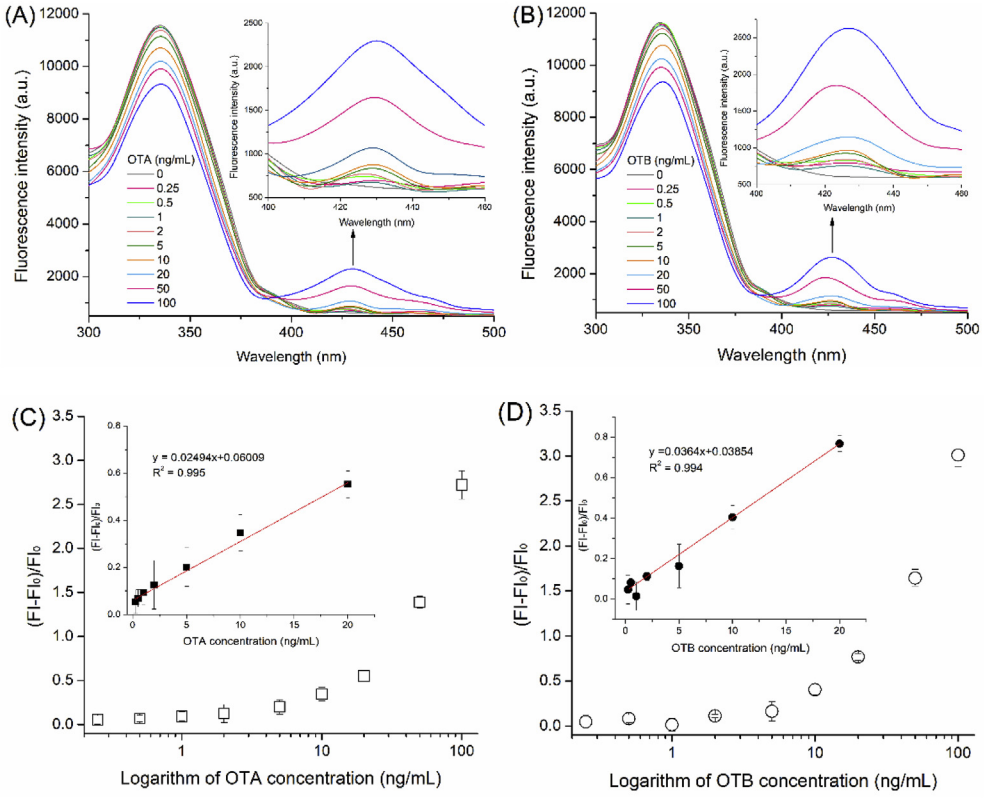

Fig. 3. Fluorescence emission spectra of solutions containing 5 μg/mL Nb28 and various concentrations of OTA (A) and OTB (B), and plot of relative fluorescence intensities $(Fl\text{-}Fl_0)/Fl_0$ at 430 nm of the antigen/Nb complex as a function of concentration of OTA (C) and OTB (D). The fluorescence spectra were recorded with excitation at 280 nm. Inset in: linear portion of the plot. The error bars indicate standard deviations of data from experiments performed in triplicate.

Table 1
Analytical performances of the Nb-based FRET immunoassay and other nanotechnology- and mass spectrometry-based assays for ochratoxins.

Protocol	Analyte	LOD	Assay time	Reference
LC–QTOF-MS	OTA	0.05 ng/mL	>45 min.	Rodríguez et al. (2016)
LC-MS/MS	OTA	0.05 ng/mL	>45 min	Meerpoel et al. (2018)
SPE-HPLC–MS/MS	OTA	0.01 ng/mL	>60 min	Campone et al. (2018)
Fluorescent aptasensor	OTA	0.8 ng/mL	190 min	He et al. (2019)
Photoelectrochemical immunosensor	OTA	0.02 pg/mL	336 min	Qileng et al. (2018)
	OTB	0.04 pg/mL		
	OTC	0.03 pg/mL		
Nb-based FRET immunoassay	OTA	0.06 ng/mL	10 min	This work
	OTB	0.12 ng/mL		

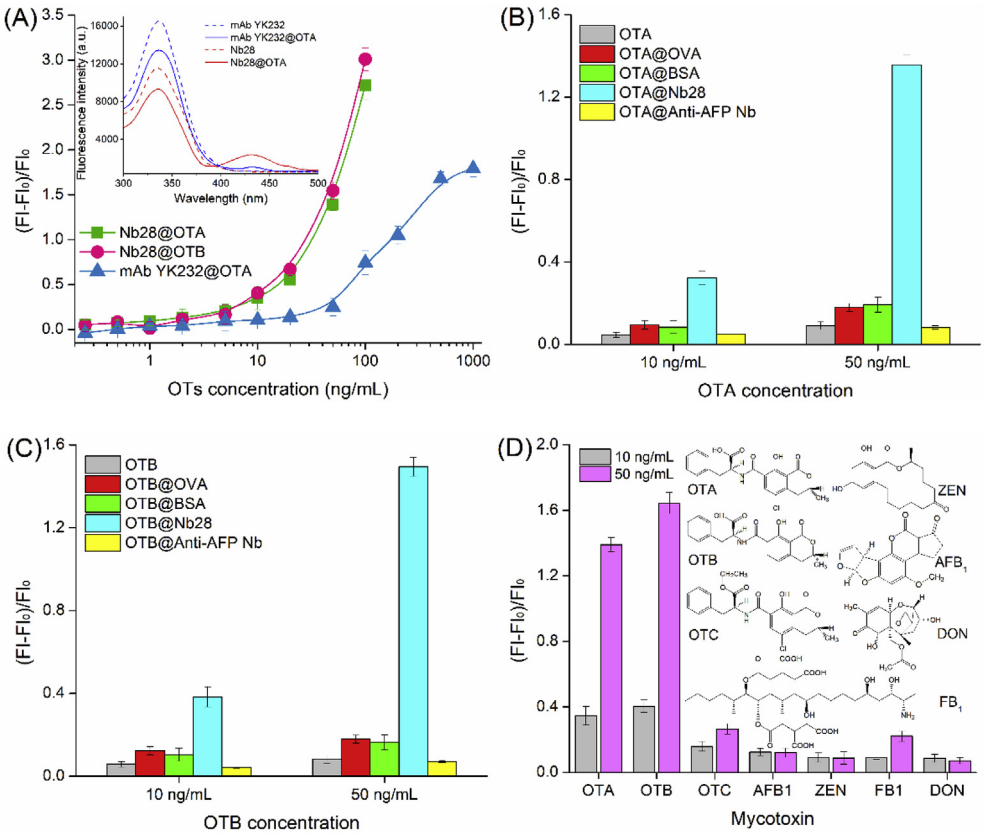

Fig. 4. Comparison of standard curves of the Nb-based FRET immunoassay for OTA and OTB and standard curve of the mAb YK232-based FRET immunoassay for OTA (A), and selectivity analysis of the Nb-based FRET immunoassay using nonspecific proteins (B and C) and structural analogues of OTA and OTB (D). The solutions containing 5 μg/mL Nb28 or 50 μg/mL mAb YK232 together with various concentrations of analyte were incubated at room temperature for 10 min. Fluorescence intensity (λ_{em}: 430 nm) of the antibody-analyte complex was recorded by excitation at 280 nm. Inset in: fluorescence emission spectra (λ_{ex}: 280 nm) of Nb28, Nb28@OTA complex, mAb YK232, and mAb YK232@OTA complex. For selectivity analysis, the nonspecific proteins including OVA (50 μg/mL), BSA (50 μg/mL), and the anti-AFP Nb (5 μg/mL) were used to replace Nb28 for incubation with 10 and 50 ng/mL OTA (A) or OTB (B). Common mycotoxins including OTC, AFB_1, ZEN, FB_1, and DON were used to replace OTA and OTB, and incubated with 5 μg/mL Nb28 (C). Fluorescence intensity (λ_{em}: 430 nm) of each solution was recorded by excitation at 280 nm. The error bars indicate standard deviations of data from experiments performed in triplicate.

0.5 ng/mL, which was 8.3 folds higher than that (0.06 ng/mL) of the Nb-based FRET immunoassay, indicating the effective way to improve the detection sensitivity of OTs using Nb.

3.4. Selectivity of the Nb-based FRET immunoassay

Several nonspecific proteins and common mycotoxins were used to replace Nb28 and target antigens (OTA and OTB) for determining the selectivity of the Nb-based FRET immunoassay. Nonspecific proteins including OVA (50 μg/mL), BSA (50 μg/mL), and the anti-AFP Nb (5 μg/mL) were subjected to the assay (Fig. 4B and C). Insignificant increases of fluorescence intensity of OTA and OTB were measured when the nonspecific proteins were incubated with 10 ng/mL and 50 ng/mL of both OTA and OTB. The fluorescence intensity caused by the binding of OVA and BSA to OTA or OTB is higher than that of the control groups containing only OTA or OTB. Nevertheless, it is much lower than that produced by the binding of Nb28 to target antigens. Furthermore, the selectivity of the Nb-based FRET immunoassay was assessed by testing the fluorescence signal of Nb28 together with the analogue of OTA and OTB (OTC) and some common mycotoxins (AFB_1, ZEN, FB_1, and DON). As shown in Fig. 4D, negligible increase of fluorescence intensity at the wavelength of 430 nm was detected for the common mycotoxins. Better interestingly, 5.7% and 58% of cross reactivity of the Nb28 with OTB and OTC (Table S-1) were detected in an Nb-based competitive heterogeneous immunoassay performed according to

the previous work (Liu et al., 2017). The results demonstrated that the increase of fluorescence intensity in the Nb-based FRET immunoassay system originated from the recognition of Nb28 to dianions of OTA and OTB in a weakly acidic buffer. Thus the developed Nb-based FRET immunoassay exhibits high selectivity for OTA and OTB.

3.5. Analysis of spiked samples by Nb-based FRET immunoassay and HPLC-FLD

The elimination or reduction of matrix effect is critical for food sample analysis. Various strategies have been successfully applied to minimize the matrix effect of food, such as dilution method and solid-phase extraction (Jiang et al., 2015; Yang et al., 2015). Dilution is the most commonly used method because of the advantages of easy operation, low cost, and speed. Nevertheless, a high dilution factor will reduce the detection sensitivity although it can effectively minimize the matrix interference. In this study, standard calibration curves using the rice sample extracts with different dilution factors were set up and compared with the one using the optimal MES-MeOH buffer (Figure S-3). There was no significant difference between the standard calibration curve without matrix and those with diluted rice sample extracts through the Student's t-test analysis at 95% confidence level ($p > 0.05$). As shown in Figure S-3, the maximum relative fluorescence intensity (FI_{max}-FI_0) decreased as the dilution factor increased. The matrix interference was effectively reduced when the dilution factor exceeded 20. Therefore, 30-fold dilution was selected to minimize the rice sample matrix effect in Nb-based FRET immunoassay system. Assay sensitivity obviously can be increased with a partition of SPE column to reduce matrix interference with an increase in assay time and cost and a decrease in reproducibility. The fluorescence enhancing rate of the mixture of Nb28 and OTA standards (2 and 10 ng/mL) prepared with 30-fold diluted rice extract (Nb28@Rice@OTA) was tested by the Nb-based FRET immunoassay, and compared with those of the control groups including the mixture of Nb28 and OTA (Nb28@OTA) and of Nb28 and rice extract (Nb28@Rice). As shown in Figure S-4, ignorable interference effect from the rice extract was observed for the detection of OTA by the Nb-based FRET immunoassay, which fortifies the concept of the proposed method.

To evaluate the effectiveness of Nb-based FRET immunoassay for real samples, the rice samples were spiked at three concentration levels of OTA (60, 150, and 300 μg/kg) for intra- and inter-assay accuracy and precision analysis and confirmed by HPLC-FLD (Table S-2). The average recoveries of OTA measured by Nb-based FRET immunoassay and HPLC-FLD were among 100–124% with the relative standard deviation (RSD) ranging from 5 to 10% and among 85–116% with RSD ranging from 4% to 9%, respectively. Furthermore, five different ratios of OTA and OTB mixtures (0:10, 8:2, 7:3, 6:4, and 5:5) at three different spiking levels (60, 150, and 300 μg/kg) were applied to the simultaneous detection of OTA and OTB by Nb-based FRET immunoassay (Table S-3). The average recovery of mixed OTs was in a range of 83–127% with RSD ranging from 3% to 11%, and the results were validated by HPLC-FLD (Table S-3). At 95% confidence level, the Student's t-test indicated that there was no significant difference in recovered OTs concentrations between the two methods ($p > 0.05$). Thus, these results revealed the acceptable accuracy and precision of Nb-based FRET immunoassay for simultaneous detection of OTA and OTB in rice samples.

4. Conclusions

In summary, we developed a noncompetitive and highly sensitive FRET-based homogeneous immunoassay system for simultaneous detection of OTA and OTB using an Nb. This system is constructed according to the following principles: Firstly, the intrinsic fluorescence energy transfers from antibody Trp residues (Donor) to antigen (Acceptor) when the specific interaction of two molecules happens. Secondly, the smaller size of Nb can contribute to the shorter mean distance between Trp residues and antigen-binding site and effective FRET distance compared to the intact antibody, and improve the fluorescence enhancing efficiency of acceptor molecule. Thus, the higher detection sensitivity is obtained in the Nb-based FRET immunoassay system. Compared to the conventional competitive ELISA systems for OTs, the new system can implement label-free, wash-free, noncompetitive, and homogeneous detection of low molecular weight compounds in a single step. These advantages can not only avoid the inactivation or activity decrease of antibody by chemical labeling method and the variability resulting from repeated washes involved in conventional ELISA, but also the FRET shortens the assay time and improves the detection sensitivity. To our knowledge, there are few reports on the simultaneous detection of OTA and OTB or other analogues using an Nb-based FRET immunoassay. Thus, this study provides model basis of highly sensitive detection of total amount of low molecular weight compounds that have similar fluorescence properties with OTA and OTB.

Acknowledgments

This work was financially supported by the National Natural Science Foundation of United States (grant number 31760493) and the Scientific Research Foundation of Hainan University (grant number kyqd1631). Partial support was provided by the National Institute of Environmental Health Sciences Superfund Research Program (grant number P42-ES04699).

Appendix A. Supplementary data

Supplementary data to this article can be found online at https://doi.org/10.1016/j.envpol.2019.04.135.

Declaration of interest statement

All authors declare no conflict of interest.

References

Al-Taher, F., Cappozzo, J., Zweigenbaum, J., Lee, H.J., Jackson, L., Ryu, D., 2017. Detection and quantitation of mycotoxins in infant cereals in the U.S. market by LC-MS/MS using a stable isotope dilution assay. Food Control 72, 27–35.

Bever, C.R.S., Majkova, Z., Radhakrishnan, R., Suni, I., McCoy, M., Wang, Y., Dechant, J., Gee, S., Hammock, B.D., 2014. Development and utilization of camelid VHH antibodies from alpaca for 2,2′,4,4′-tetrabrominated diphenyl ether detection. Anal. Chem. 86, 7875–7882.

Borkman, R.F., Lerman, S., 1978. Fluorescence spectra of tryptophan residues in human and bovine lens proteins. Exp. Eye Res. 26, 705–713.

Campone, L., Piccinelli, A.L., Celano, R., Pagano, I., Russo, M., Rastrelli, L., 2018. Rapid and automated on-line solid phase extraction HPLC–MS/MS with peak focusing for the determination of ochratoxin A in wine samples. Food Chem. 244, 128–135.

Di Stefano, V., Pitonzo, R., Avellone, G., Di Fiore, A., Monte, L., Ogorka, A.Z.T., 2015. Determination of aflatoxins and ochratoxins in Sicilian sweet wines by high-performance liquid chromatography with fluorometric detection and immunoaffinity cleanup. Food Anal. Methods 8, 569–577.

Gan, F., Zhou, Y., Qian, G., Huang, D., Hou, L., Liu, D., Chen, X., Wang, T., Jiang, P., Lei, X., Huang, K., 2018. PCV2 infection aggravates ochratoxin A-induced nephrotoxicity via autophagy involving p38 signaling pathway in vivo and in vitro. Environ. Pollut. 238, 656–662.

Gareis, M., Gareis, E., 2007. Guttation droplets of Penicillium nordicum and Penicillium verrucosum contain high concentrations of the mycotoxins ochratoxin A and B. Mycopathologia 163, 207–214.

Greenberg, A.S., Avila, D., Hughes, M., Hughes, A., McKinney, E.C., Flajnik, M.F., 1995. A new antigen receptor gene family that undergoes rearrangement and

extensive somatic diversification in sharks. Nature 374, 168–173.
Hamers-Casterman, C., Atarhouch, T., Muyldermans, S., Robinson, G., Hammers, C., Songa, E.B., Bendahman, N., Hammers, R., 1993. Naturally occurring antibodies devoid of light chains. Nature 363, 446–448.
Harmsen, M.M., De Haard, H.J., 2007. Properties, production, and applications of camelid single-domain antibody fragments. Appl. Microbiol. Biotechnol. 77, 13–22.
Hashemi, J., Alizadeh, N., 2009. Investigation of solvent effect and cyclodextrins on fluorescence properties of ochratoxin A. Spectrochim. Acta, Part A 73, 121–126.
He, T., Wang, Y., Li, P., Zhang, Q., Lei, J., Zhang, Z., Ding, X., Zhou, H., Zhang, W., 2014. Nanobody-based enzyme immunoassay for aflatoxin in agro-products with high tolerance to cosolvent methanol. Anal. Chem. 86, 8873–8880.
He, Y., Tian, F., Zhou, J., Jiao, B., 2019. A fluorescent aptasensor for ochratoxin A detection based on enzymatically generated copper nanoparticles with a polythymine scaffold. Microchim. Acta 186 (3), 199–205.
Huo, J., Li, Z., Wan, D., Li, D., Qi, M., Barnych, B., Vasylieva, N., Zhang, J., Hammock, B.D., 2018. Development of a highly sensitive direct competitive fluorescence enzyme immunoassay based on a nanobody–alkaline phosphatase fusion protein for detection of 3-phenoxybenzoic acid in urine. J. Agric. Food Chem. 66, 11284–11290.
Il'ichev, Y.V., Perry, J.L., Manderville, R.A., Chignell, C.F., Simon, J.D., 2001. The pH-dependent primary photoreactions of ochratoxin A. J. Phys. Chem. B 105, 11369–11376.
Il'ichev, Y.V., Perry, J.L., Simon, J.D., 2002. Interaction of ochratoxin a with human serum albumin. Preferential binding of the dianion and pH effects. J. Phys. Chem. B 106, 452–459.
Jiang, R., Xu, J., Zhu, F., Luan, T., Zeng, F., Shen, Y., Ouyang, G., 2015. Study of complex matrix effect on solid phase microextraction for biological sample analysis. J. Chromatogr. A 1411, 34–40.
Kim, H., McCoy, M., Gee, S.J., González-Sapienza, G.G., Hammock, B.D., 2011. Noncompetitive phage anti-immunocomplex real-time polymerase chain reaction for sensitive detection of small molecules. Anal. Chem. 83, 246–253.
Lakowicz, J.R., 1999. Instrumentation for Fluorescence Spectroscopy, Principles of Fluorescence Spectroscopy. Springer US, Boston, MA, pp. 25–61.
Lee, J., Lim, W., Ryu, S., Kim, J., Song, G., 2019. Ochratoxin A mediates cytotoxicity through the MAPK signaling pathway and alters intracellular homeostasis in bovine mammary epithelial cells. Environ. Pollut. 246, 366–373.
Li, T., Byun, J., Kim, B.B., Shin, Y., Kim, M., 2013. Label-free homogeneous FRET immunoassay for the detection of mycotoxins that utilizes quenching of the intrinsic fluorescence ofantibodies. Biosens. Bioelectron. 42, 403–408.
Liang, Y., Huang, X., Yu, R., Zhou, Y., Xiong, Y., 2016. Fluorescence ELISA for sensitive detection of ochratoxin A based on glucose oxidase-mediated fluorescence quenching of CdTe QDs. Anal. Chim. Acta 936, 195–201.
Lim, S., Ichinose, H., Shinoda, T., Ueda, H., 2007. Noncompetitive detection of low molecular weight peptides by open sandwich immunoassay. Anal. Chem. 79, 6193–6200.
Liu, X., Tang, Z., Duan, Z., He, Z., Shu, M., Wang, X., Gee, S.J., Hammock, B.D., Xu, Y., 2017. Nanobody-based enzyme immunoassay for ochratoxin A in cereal with high resistance to matrix interference. Talanta 164, 154–158.
Liu, X., Xu, Y., Wan, D., Xiong, Y., He, Z., Wang, X., Gee, S.J., Ryu, D., Hammock, B.D., 2015. Development of a nanobody–alkaline phosphatase fusion protein and its application in a highly sensitive direct competitive fluorescence enzyme immunoassay for detection of ochratoxin a in cereal. Anal. Chem. 87, 1387–1394.
Liu, X., Xu, Y., Xiong, Y., Tu, Z., Li, Y., He, Z., Qiu, Y., Fu, J., Gee, S.J., Hammock, B.D., 2014. VHH phage-based competitive real-time immuno-polymerase chain reaction for ultrasensitive detection of ochratoxin a in cereal. Anal. Chem. 86, 7471–7477.
Masters, B.R., 2014. Paths to Förster's resonance energy transfer (FRET) theory. Eur. Phys. J. H 39, 87–139.
Meerpoel, C., Vidal, A., di Mavungu, J.D., Huybrechts, B., Tangni, E.K., Devreese, M., Croubels, S., De Saeger, S., 2018. Development and validation of an LC–MS/MS method for the simultaneous determination of citrinin and ochratoxin a in a variety of feed and foodstuffs. J. Chromatogr. A 1580, 100–109.
Muyldermans, S., 2013. Nanobodies: natural single-domain antibodies. Annu. Rev. Biochem. 82, 775–797.
Qileng, A., Wei, J., Lu, N., Liu, W., Cai, Y., Chen, M., Lei, H., Liu, Y., 2018. Broad-specificity photoelectrochemical immunoassay for the simultaneous detection of ochratoxin A, ochratoxin B and ochratoxin C. Biosens. Bioelectron. 106, 219–226.
Remiro, R., Ibáñez-Vea, M., González-Peñas, E., Lizarraga, E., 2010. Validation of a liquid chromatography method for the simultaneous quantification of ochratoxin A and its analogues in red wines. J. Chromatogr. A 1217, 8249–8256.
Rodríguez-Cabo, T., Rodríguez, I., Ramil, M., Cela, R., 2016. Liquid chromatography quadrupole time-of-flight mass spectrometry selective determination of ochratoxin A in wine. Food Chem. 199, 401–408.
Schreiber, A.B., Strosberg, A.D., Pecht, I., 1978. Fluorescence of tryptophan residues in homogeneous rabbit antibodies: variability in quantum yields and degree of exposure to solvent. Immunochemistry 15, 207–212.
Sun, Z., Duan, Z., Liu, X., Deng, X., Tang, Z., 2017. Development of a nanobody-based competitive dot ELISA for visual screening of ochratoxin a in cereals. Food Anal. Methods 10, 3558–3564.
Sun, Z., Lv, J., Liu, X., Tang, Z., Wang, X., Xu, Y., Hammock, B.D., 2018. Development of a nanobody-AviTag fusion protein and its application in a streptavidin–biotin-amplified enzyme-linked immunosorbent assay for ochratoxin a in cereal. Anal. Chem. 90, 10628–10634.
Sun, Z., Wang, X., Tang, Z., Chen, Q., Liu, X., 2019. Development of a biotin-streptavidin-amplified nanobody-based ELISA for ochratoxin A in cereal. Ecotoxicol. Environ. Saf. 171, 382–388.
Tang, Z., Wang, X., Lv, J., Hu, X., Liu, X., 2018. One-step detection of ochratoxin A in cereal by dot immunoassay using a nanobody-alkaline phosphatase fusion protein. Food Control 92, 430–436.
Tao, Y., Xie, S., Xu, F., Liu, A., Wang, Y., Chen, D., Pan, Y., Huang, L., Peng, D., Wang, X., Yuan, Z., 2018. Ochratoxin A: toxicity, oxidative stress and metabolism. Food Chem. Toxicol. 112, 320–331.
Tyagi, S., Marras, S.A.E., Kramer, F.R., 2000. Wavelength-shifting molecular beacons. Nat. Biotechnol. 18, 1191.
Wang, J., Bever, C.R.S., Majkova, Z., Dechant, J.E., Yang, J., Gee, S.J., Xu, T., Hammock, B.D., 2014. Heterologous antigen selection of camelid heavy chain single domain antibodies against tetrabromobisphenol A. Anal. Chem. 86, 8296–8302.
Xiao, H., Madhyastha, S., Marquardt, R.R., Li, S., Vodela, J.K., Frohlich, A.A., Kemppainen, B.W., 1996. Toxicity of ochratoxin A, its opened lactone form and several of its analogs: structure–activity relationships. Toxicol. Appl. Pharmacol. 137, 182–192.
Xu, W., Xiong, Y., Lai, W., Xu, Y., Li, C., Xie, M., 2014. A homogeneous immunosensor for AFB_1 detection based on FRET between different-sized quantum dots. Biosens. Bioelectron. 56, 144–150.
Yang, P., Chang, J.S., Wong, J.W., Zhang, K., Krynitsky, A.J., Bromirski, M., Wang, J., 2015. Effect of sample dilution on matrix effects in pesticide analysis of several matrices by liquid chromatography–high-resolution mass spectrometry. J. Agric. Food Chem. 63, 5169–5177.